Original Paper

Neuro
-endocrinology

Neuroendocrinology 2019;109:374–390
DOI: 10.1159/000500201

Received: February 4, 2019
Accepted after revision: April 2, 2019
Published online: April 16, 2019

Persistent Leptin Signaling in the Arcuate Nucleus Impairs Hypothalamic Insulin Signaling and Glucose Homeostasis in Obese Mice

Eglantine Balland[a] Weiyi Chen[a] Tony Tiganis[b] Michael A. Cowley[a]

[a]Department of Physiology, Metabolism, Diabetes and Obesity Program, Biomedicine Discovery Institute, Monash University, Clayton, VIC, Australia; [b]Department of Biochemistry and Molecular Biology , Metabolism, Diabetes and Obesity Program, Biomedicine Discovery Institute, Monash University, Clayton, VIC, Australia

Keywords
Diabetes · Hypothalamus · Insulin resistance · Leptin · Obesity

Abstract
Background: Obesity is associated with reduced physiological responses to leptin and insulin, leading to the concept of obesity-associated hormonal resistance. ***Objectives:*** Here, we demonstrate that contrary to expectations, leptin signaling not only remains functional but also is constantly activated in the arcuate nucleus of the hypothalamus (ARH) neurons of obese mice. This state of persistent response to endogenous leptin underpins the lack of response to exogenous leptin. ***Methods and Results:*** The study of combined leptin and insulin signaling demonstrates that there is a common pool of ARH neurons responding to both hormones. More importantly, we show that the constant activation of leptin receptor neurons in the ARH prevents insulin signaling in these neurons, leading to impaired glucose tolerance. Accordingly, antagonising leptin signaling in diet-induced obese (DIO) mice restores insulin signaling in the ARH and improves glucose homeostasis. Direct inhibition of PTP1B in the CNS restores arcuate insulin signaling similarly to leptin inhibition; this effect is likely to be mediated by AgRP neurons since PTP1B deletion specifically in AgRP neurons restores glucose and insulin tolerance in DIO mice. ***Conclusions:*** Finally, our results suggest that the constant activation of arcuate leptin signaling in DIO mice increases PTP1B expression, which exerts an inhibitory effect on insulin signaling leading to impaired glucose homeostasis.

Introduction

Leptin is produced by adipocytes and instructs the brain on energy stores to regulate energy balance accordingly [1, 2]. Circulating leptin levels are proportionate to adiposity level [3]. From the blood, leptin enters the brain [4, 5] and signals via its leptin receptor (LepRb), present in various brain regions and highly expressed within the arcuate nucleus of the hypothalamus (ARH) [6, 7]. LepRb neuronal signaling in the ARH is coordinated via the signal transducer and activator of transcription 3 (STAT3) and protein kinase B/Akt pathways [8] and when activated reduces food intake and body weight [9, 10]. Importantly, obesity is associated with a high level of circu-

E-Mail karger@karger.com
www.karger.com/nen

Dr. Eglantine Balland and Prof. Michael A. Cowley
Department of Physiology, Metabolism, Diabetes and Obesity Program
Biomedicine Discovery Institute, Monash University
26 Innovation Walk, Clayton, VIC 3800 (Australia)
E-Mail eglantine.balland@monash.edu and michael.cowley@monash.edu

lating leptin, or hyperleptinemia. However, obesity is characterized by the absence of an adequate response to the high level of endogenous leptin [11], this particular state is known as "leptin resistance." Recent evidence indicates that some leptin activity persists in obesity [12, 13]. Leptin has profound effect on body weight regulation and glucose homeostasis [14–17]. Obesity is associated with hyperleptinemia, hyperglycemia, hyperinsulinemia and type 2 diabetes. Besides leptin actions in the ARH, insulin also activates the phospho-inositol-3-kinase/Akt signaling cascade through central insulin receptor (InsR) to maintain normal glucose homeostasis [18]. Insulin resistance in the brain occurs in obesity and may be involved in type 2 diabetes pathogenesis. Furthermore, recent studies also link central insulin resistance with depression and neurodegenerative diseases [19, 20].

In the present study, we aim to define the state of "leptin resistance" at the cellular level diet-induced obese (DIO) mice and its possible involvement in glucose homeostasis impairment. DIO mice display a constant high basal LepRb signaling in the ARH owing to the presence of hyperleptinemia and this is characterized by sustained activation of both STAT3 and Akt signaling pathways. We hypothesized that the elevated LepRb signaling in DIO mice is associated with attenuated insulin signaling, contributing to the alteration of glucose homeostasis. This study redefines our understanding of central leptin resistance and highlights a previously unexplored mechanism by which leptin signaling perturbs the central control of glucose metabolism in diet-induced obesity, defining a possible molecular link between hyperleptinemia-induced neuronal signaling and central insulin resistance.

Materials and Methods

Animals

All animal procedures were approved by Monash University Animal Ethics Committee. Two- to three-month-old male C57BL6 mice (Monash Animal Services) were housed in a controlled environment with constant temperature and 12 h light/12 h dark cycle in a high-barrier facility (Monash ARL). Mice were either fed ad libitum with standard chow diet (8.5% fat, Barastoc, Ridley AgriProducts, Australia) or high-fat diet (HFD; 43% energy from fat, SF04–001, Specialty Feeds, Western Australia, Australia) for 12–20 weeks. To generate Agrp-Ires-Cre; $Ptpn1^{fl/fl}$ (AgRP-1B), $Ptpn1^{fl/fl}$ (C57BL/6) mice [21] were bred with Agrp-Ires-Cre mice [22].

Genotyping

Genotyping was performed by PCR on DNA extracted from tail biopsies using primers previously described for the Agrp-Ires-Cre [22] and $Ptpn1^{fl/fl}$ *mice* [21].

Lateral Ventricle Cannulation and Intracerebro-Ventricular Infusions

Cannulas were stereotaxically inserted (1.0 mm lateral and 0.2 mm rostral to bregma). Each surgery was followed by 1 week of recovery before performing additional procedures on cannulated mice. For the brain signaling analysis, recombinant murine leptin (1 μg; Peprotech), leptin antagonist (LAN; 5 μg; Protein Laboratories Rehovot, Israel), cucurbitacin (5 μg; Sigma-Aldrich), or claramine (5 μg; Sigma-Aldrich) were infused 30 min before paraformaldehyde intracardiac perfusion.

Antibodies used for IHC

pSTAT3 (1:1,000; Cell Signaling Technology #9131, USA)
pAkt (1:1,000; Cell Signaling Technology #4060, USA)
γ-MSH (1:1,000; Antibodies Australia #AS599, Australia)
AgRP (1:1,000; Antibodies Australia #AS506, Australia)

Immunofluorescence

Mice were fasted overnight and injected peripherally in the morning with saline, with leptin (3 mg/kg; Peprotech) 45 min before perfusion or with insulin (5 units/mouse; Novo Nordisk) 10 min before perfusion. Intracardiac perfusions were performed on isofluorane-anaesthetized mice with 2% paraformaldehyde. Brains were postfixed, cryoprotected overnight at 4 °C in a 20% sucrose solution, and embedded in Tissue Tek (Miles, Elkhart, IN, USA) before freezing. Thirty micro meter-thick coronal sections were cut on a cryostat and processed for immunofluorescence as previously described [5, 23]. Since pSTAT3 and pAkt antibodies were produced in the same specie (rabbit), we used a sequential staining protocol with a fixation step between the 2 primary antibodies. pSTAT3 antibody was incubated first for 48 h at 4 °C and subsequently incubated with a goat-anti-rabbit Alexa 568. After revelation of pSTAT3 in red, slices were extensively washed in KPBS and then fixed with 4% PFA for 1 min. Following the fixation step, brain slices were washed in KPBS and incubated with pAkt antibody for 48 h at 4 °C. Slices were then revealed using goat-anti-rabbit Alexa 488 green secondary antibody, washed and coversliped. Figure 3c illustrates the specificity of our signal and the absence of cross-reactivity that would have generated 100% of co-localization.

Double-immunofluorescence images were acquired using a confocal microscope (Leica SP8 Confocal Invert, Monash Microimaging). The number of immunoreactive cells was counted using Image J software in three hemi-sections of similar rostro-caudal level (bregma –1.82 to –2.06) per mouse (see next section for more details).

Immunohistochemistry Images Quantification

Microphotographs were taken on a confocal microscope with the same settings. Unmodified pictures (no modification of contrast, brightest or any other parameter, no threshold applied) were subjected to quantification using Image J software (point tool) on individual channel images. Neurons were considered as specifically labeled when the same researcher was able to clearly identify a colored neuron (green or red) at a fixed distance from the screen (50 cm) on pictures displayed at the same zoom level. Each labeled neuron was marked with a colored dot (green dot on pAkt-labeled neurons placed on green channel picture; red dot on pSTAT3-labeled neurons placed on red channel picture). After completion of neurons quantification on individual channel picture, the dots

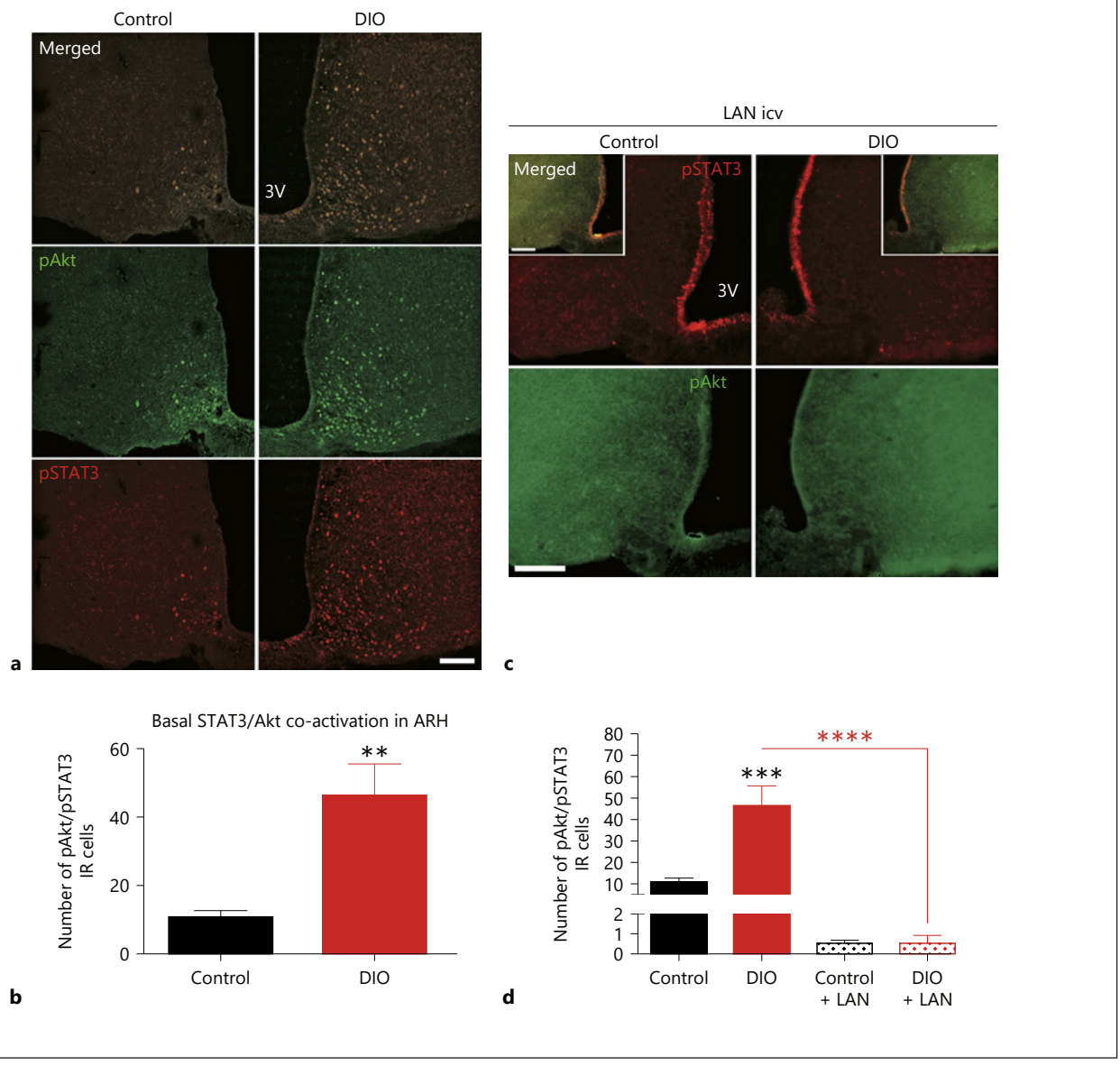

Fig. 1. DIO mice display high levels of STAT3 and Akt activation in the ARH in basal conditions, which is suppressed by centrally delivered LAN. **a** Representative photomicrographs (10×) showing pSTAT3 (red) and pAkt (green)-labeled cells following ip saline injection (scale bar 75 μm). The doted lines represent the region of labeled neurons quantification. **b** Graph representing the mean number of ARH neurons colabeled for pSTAT3 and pAkt per hemi-section 30 min after saline ip injection. **c** Representative photomicrographs (10×) showing pSTAT3 labeled cells (red) and pAkt labeled cells (green) 30 min following LAN injection (5 μg) in the LV. STAT3 and Akt basal coactivation is suppressed in control diet mice and DIO mice (scale bar 75 μm). Arrowheads highlight examples of pSTAT3-alone (red) and pAkt-alone (green) neurons. **d** Graph representing the mean number of ARH neurons displaying pSTAT3/pAkt colabeled cells per hemi-section in basal conditions or 30 min after LAN icv injection. All data are represented as mean SEM ($n = 4$ mice/group). ns, $p > 0.05$; ** $p < 0.01$; *** $p < 0.001$; **** $p < 0.0001$ as determined by two-tailed unpaired t test (**b**) and one-way ANOVA followed by Tukey's post hoc test (**d**). See also online suppl. Figure S1 and S2. LAN, leptin antagonist; icv, intracerebro-ventricular; DIO, diet-induced obese; STAT3, signal transducer and activator of transcription; ARH, arcuate nucleus of the hypothalamus.

were pasted on the picture ("flatten" option from the Image tab on Image J). In order to quantify consistently and accurately the co-localizations of pAkt and pSTAT3 staining, individual channels pictures displaying colored dots (pAkt-labeled neurons with green dots and pSTAT3-labeled neurons with red dots) were opened on illustrator software. The transparency level of the pictures was set to 40% and then the green and red channel pictures were superposed, allowing the quantification of green dots alone (pAkt-alone), red dots alone (pSTAT3-alone), and colocalized green and red dots (pakt/pSTAT3 colocalization).

NB: The same quantification method was used for triple labeling. The quantification area (ARH) was identified by the detection of the ARH boundaries by the observation of cell nuclei autofluorescence or cell nucleus counterstaining using Hoechst. The researcher was blind to the treatments and performed a second quantification on several pictures (minimum 4 per experiment) on a different day to ensure the consistency of the quantification. The differences between both quantifications were consistently inferior to 5%. Figure 3c and online suppl. Fig. 3 (for all online suppl. material, see www.karger.com/doi/10.1159/000500201).

Ex vivo Experiments

Mice fed with standard chow or HFD for 15–20 weeks were fasted overnight prior being anesthetized with isofluorane to receive an intracardiac perfusion of cold aCSF. Then brains were quickly extracted and cut in 150 μm slices, using a vibratome. Brain slices were collected from –1.34 to –2.30 mm relative to bregma. After 1 h of recovery during which slices were placed in aCSF oxygenized with carbogen, they were incubated in fresh aCSF with saline (1 μL) or in fresh aCSF with leptin (100 nM; Peprotech) for 45 min at room temperature. At the end of the treatment, slices were fixed by immersion in 2% PFA and stored at –20 °C in cryoprotective solution until being proceeded. Immunofluorescence was performed on the slices using the same protocol used for in vivo immunostaining. In this experiment, 6 control and 6 DIO mice were used for the pSTAT3/γ-MSH colabeling and another group of 6 control and 6 DIO mice for the pSTAT3/AgRP colabeling.

Metabolic Measurements

Glucose tolerance tests (GTTs) and insulin tolerance tests were performed on 16 h (Fig. 4e, f), 6 h (Fig. 6h, i), and 4 h (Fig. 6j, k) fasted conscious mice by injecting D-glucose (2 mg/g body weight) or insulin (0.65 mU/g body weight) into the peritoneal cavity and measuring glucose in tail blood immediately before and at 15, 30, 60, 90, and 120 min after intraperitoneal (ip) injection using an Accu-Check glucometer (Roche, Germany). The 7 days of LAN or aCSF injections prior GTT were performed as follow: 5 μg, once daily, 1 h before dark phase. The GTT was performed on day 8, 16 h following the last injection.

Body composition (lean and fat mass) was measured using EchoMRI (Echo Medical Systems, Houston, TX, USA).

Statistics

Data were analyzed on GraphPad PRISM and are represented as mean with error bars indicating SEM. p values were calculated using one-way ANOVA followed by Tukey's multiple-comparison test, two-way ANOVA followed by Bonferroni's post hoc test, or t test. ns, $p > 0.05$; * $p < 0.05$; ** $p < 0.01$; *** $p < 0.001$; **** $p < 0.0001$.

Results

Persistent Leptin Signaling in Arcuate Neurons in DIO Mice

After 12 weeks on HFD mice had increased body weight compared to chow fed mice (online suppl. Fig. S1a). When leptin was delivered into the lateral ventricle of control mice (intracerebro-ventricular injection, or icv), we observed an increase in the number of pSTAT3-labeled neurons, but this effect was absent in obese mice (online suppl. Fig. S1b). ip injection of leptin did not increase the number of pSTAT3-labeled neurons in the ARH of DIO mice. However, in basal conditions, DIO mice express a higher number of pSTAT3-labeled neurons in the ARH compared to lean, chow fed mice (Fig. 1b; online suppl. Fig. S1c), confirming previous findings [23].

We also performed a combined immunostaining for pSTAT3 and pAkt without exogenous leptin stimulation in control and DIO mice. DIO mice displayed an increase in both pSTAT3-labeled and pAkt-labeled neurons in the basal state when compared to control mice. Importantly, most of the pSTAT3-labeled ARH neurons were also pAkt-labeled (Fig. 1a, b). The coactivation of 2 LepRb-associated signaling pathways suggests that endogenous leptin may be responsible for the high basal activation of STAT3 and Akt in the ARH of DIO mice.

To test if hyperleptinemia drives constant LepRb activation in ARH neurons, we injected control and DIO mice icv with LAN [24] to block endogenous leptin from activating LepRb-associated signaling pathways (Fig. 1c). In DIO mice, we observed a striking decrease in the number of neurons that were labeled for both pSTAT3 and pAkt. LAN virtually abolished STAT3 and Akt coactivation in ARH neurons (Fig. 1d). Interestingly, the degree of pSTAT3 and pAkt colocalized expression was similar between control and DIO mice after LAN injection (Fig. 1d; online suppl. Fig. S2b). This is consistent with the notion that endogenous leptin in DIO mice is responsible for most of the STAT3 and Akt coactivation seen in ARH neurons.

Leptin-Induced pSTAT3 in ARH Neurons in Ex vivo Hypothalamic Slices from DIO Mice

To determine whether LepR-expressing neurons in the ARH of DIO mice remain responsive to leptin, we incubated hypothalamic slices from DIO mice ex vivo with vehicle or 100 nM leptin and monitored for leptin signaling by staining for pSTAT3. Using this approach, we abrogated the hyperleptinemic environment of hypothalami in DIO and investigated the response of ARH neurons to exogenous leptin in brain slices taken from lean and

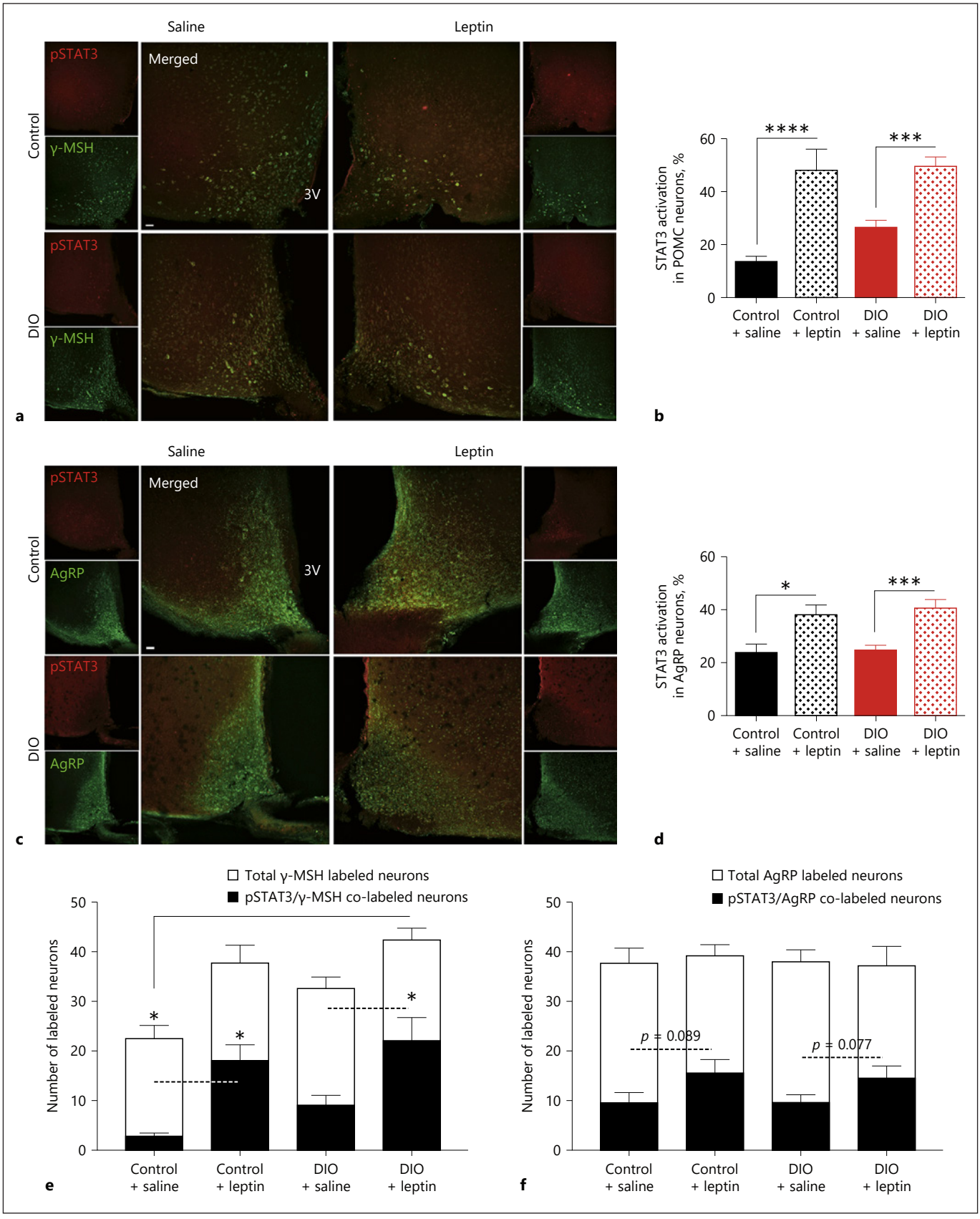

2

(For legend see next page.)

DIO mice. Following a 1 h recovery time, 6 whole brain slices (150 μm/slice) containing ARH neurons were obtained from each mouse and placed in fresh medium. Of the 6 slices, 3 slices were incubated in aCSF with saline while the other 3 were incubated in aCSF containing leptin (100 nM) for 45 min. Slices were then fixed and immunohistochemistry for pSTAT3 was used to quantify cellular responses to saline and exogenous leptin in proopiomelanocortin (POMC) and AgRP neurons (Fig. 2). γ-MSH is a peptide derived from the POMC precursor, less studied than α-MSH, another POMC precursor, well known for its appetite suppressive action. However, γ-MSH offers the advantage to be easily detectable by immunostaining compared to α-MSH, which is released too rapidly to be observed in the cytoplasm of POMC neurons. Therefore, we decided to use γ-MSH as a marker of POMC neurons. Specifically, leptin-activated POMC neurons were stained for pSTAT3 (red) and γ-MSH (green) and the number of pSTAT3-labeled, γ-MSH-labeled, and pSTAT3/γ-MSH-double labeled cells quantified. Similarly, AgRP neurons were stained for pSTAT3 (red) and AgRP (green) and the number of pSTAT3-labeled, AgRP-labeled, and pSTAT3/AgRP-double labeled cells quantified. Interestingly, we found that the level of pSTAT3 did not differ between control and DIO mice under basal conditions in POMC and AgRP neurons, respectively (Fig. 2b, d). However, pSTAT3-labeled POMC (Fig. 2a, b) and AgRP (Fig. 2c, d) neurons were elevated similarly in control and DIO mice in the presence of exogenous leptin. These results indicate that ARH POMC and AgRP neurons remain responsive to leptin in DIO. Moreover, these results are in line with the idea that hyperleptinemia in obesity may account for the high basal pSTAT3 signaling (see also Fig. 2e, f).

Persistent ARH Leptin-Signaling and Diminished Insulin Signaling in DIO

Since leptin is capable of coactivating Akt and STAT3 signaling within the same cell, we used it to discriminate between the respective actions of leptin (pAkt/pSTAT3 colabeled cells) and insulin (pAkt-alone labeled cells, not colocalized with pSTAT3) within the ARH (Fig. 1c for illustration of pAkt-alone and pAkt/pSTAT3 colabeled neurons). Importantly, exogenous insulin or leptin injection induced a similar increase in the number of pAkt-alone labeled cells and pSTAT3/pAkt colabeled cells in the ARH of lean mice, respectively (Fig. 3a, b, d for schematic representation of quantification method). Interestingly, the number of pSTAT3/pAkt colabeled and pAkt-alone labeled neurons was significantly increased upon leptin and insulin coinjection compared to saline injection. However, the magnitude of the increase in number of pAkt-alone labeled and pSTAT3/pAkt colabeled neurons was markedly attenuated compared to a single injection of either insulin or leptin (Fig. 3a, b). This suggests the existence of a common pool of ARH neurons that responds to both leptin and insulin. In DIO mice, the number of pAkt-alone labeled neurons remained unaltered upon ip insulin injection (Fig. 4a, b; online suppl. Fig. S2a). In line with our earlier findings, DIO mice display a higher number of pSTAT3/pAkt colabeled neurons when compared to age matched control mice after saline injection (Fig. 1a, b, 4a, d), the number of pSTAT3/pAkt-labeled neurons was also unchanged after insulin injection (Fig. 4a, d; online suppl. Fig. S2a). Noteworthy, hypothalamic insulin signaling mostly occurred in the ARH (online suppl. Fig. S1d).

In DIO mice, it is evident that a large population of leptin-sensitive neurons in the ARH are responsive to endogenous leptin in the basal state and this reduces the action of exogenous leptin (online suppl. Fig. S1b, S2a) or insulin (Fig. 4a, b; online suppl. Fig. S2a) on these neu-

Fig. 2. Ex vivo slices from DIO mice display leptin-induced pSTAT3. **a** Representative photomicrographs (20×) of ex vivo slices from control and DIO mice showing γ-MSH-labeled cells (green) and pSTAT3-labeled cells (red) following 45 min incubation in aCSF + saline or in aCSF + 100 nM leptin (scale bar 25 μm, merged image). **b** Graph representing the percentage of pSTAT3 labeling in γ-MSH-expressing ARH neurons following 45 min incubation of the slices in aCSF + saline or in aCSF + 100 nM leptin. **c** Representative photomicrographs (20×) of ex vivo slices from control and DIO mice showing AgRP-labeled cells (green) and pSTAT3-labeled cells (red) following 45 min incubation in aCSF + saline or in aCSF + 100 nM leptin (scale bar 25 μm, merged image). **d** Graph representing the percentage of pSTAT3 labeling in AgRP-expressing ARH neurons following 45 min incubation of the slices in aCSF + saline or in aCSF + 100 nM leptin. **e** Graph representing the mean number of cells displaying γ-MSH/pSTAT3 colocalization within the total number of γ-MSH-labeled cells. **f** Graph representing the mean number of cells displaying AgRP/pSTAT3 colocalization within the mean number of total AgRP-labeled cells. All data are represented as mean SEM ($n = 4$ control diet and 6 DIO mice). * $p < 0.05$; *** $p < 0.001$; **** $p < 0.0001$ as determined by one-way ANOVA followed by Tukey's post hoc test (**b**, **d**–**f**). DIO, diet-induced obese; STAT3, signal transducer and activator of transcription; POMC, proopiomelanocortin.

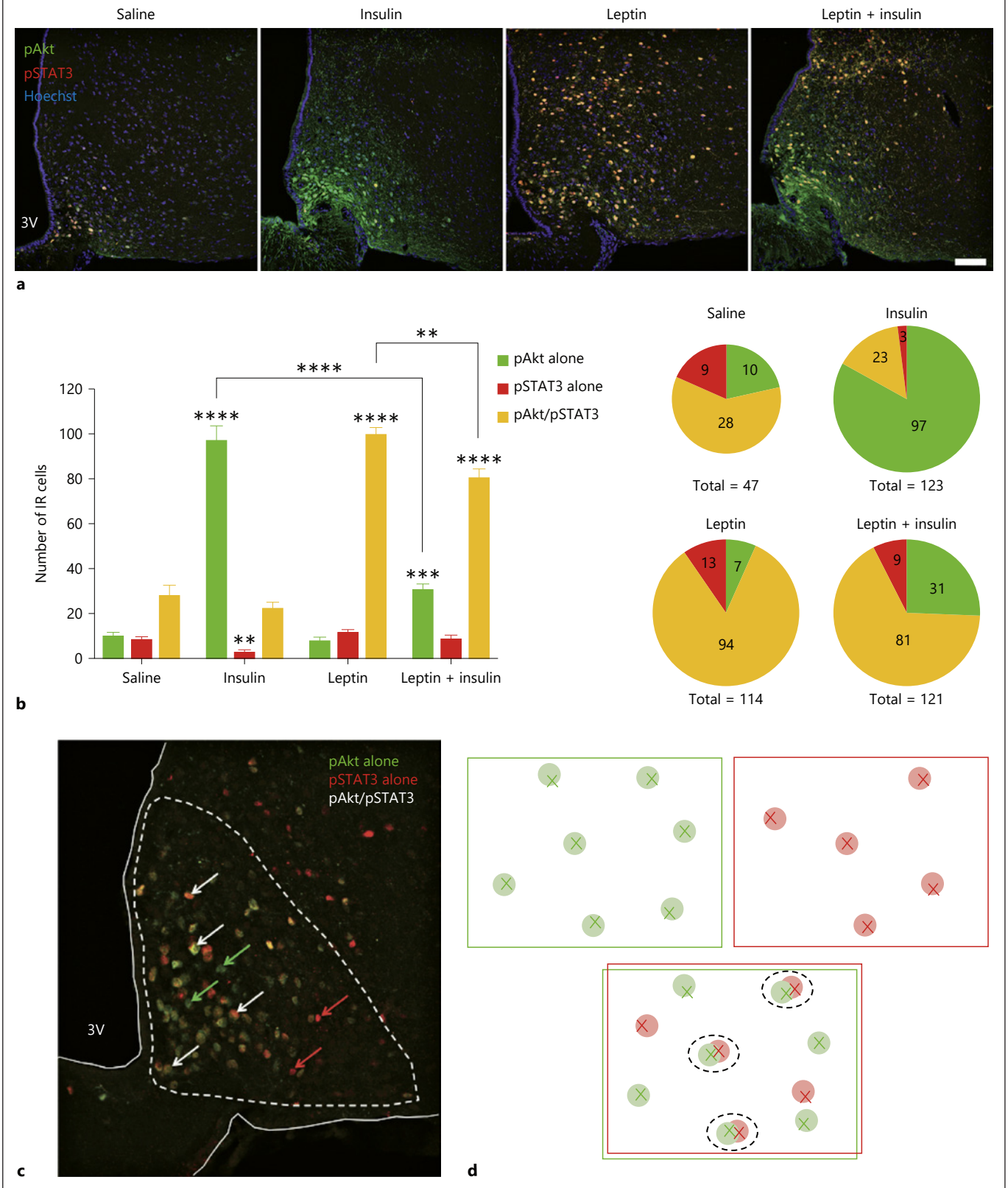

3

(For legend see next page.)

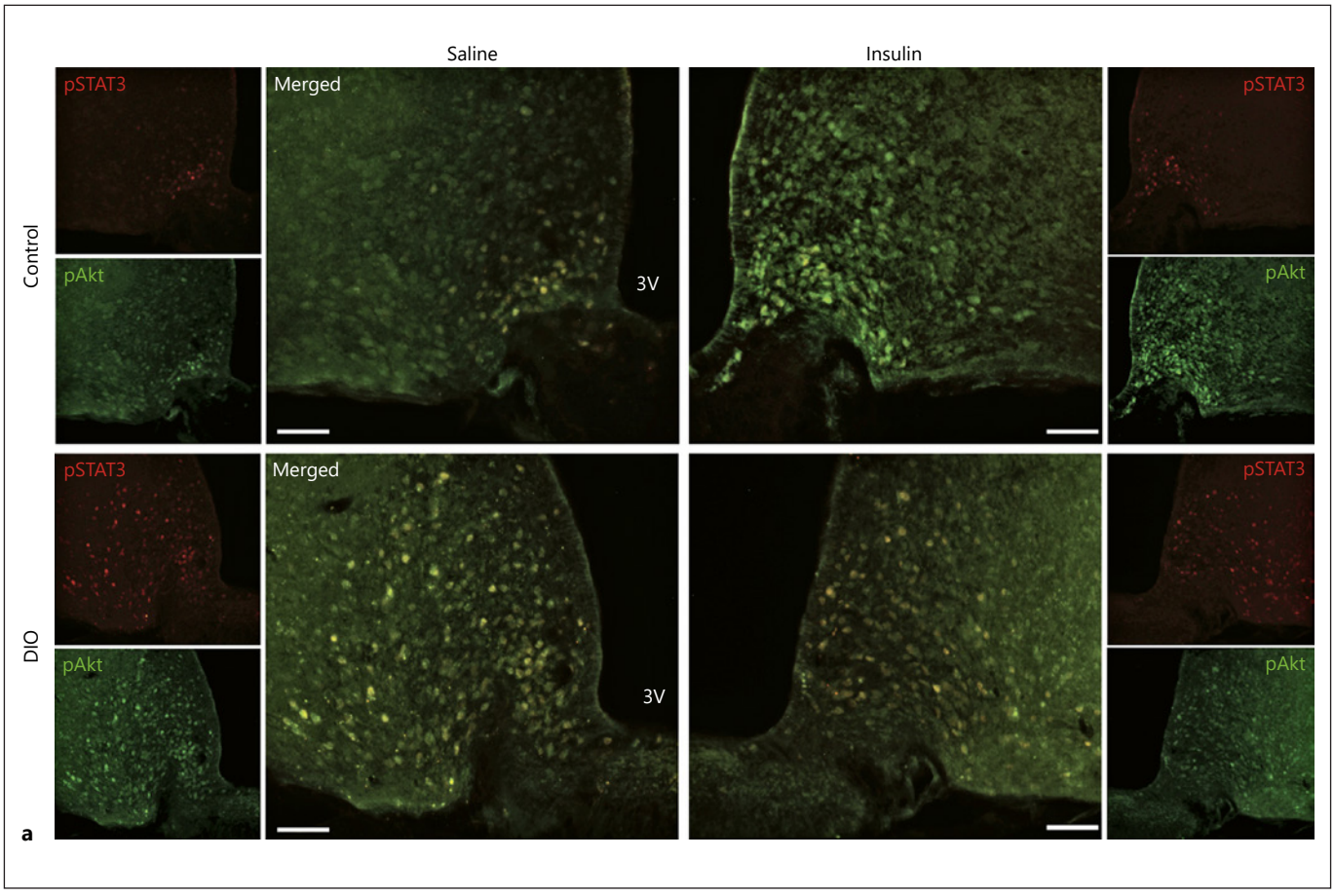

Fig. 4. Centrally delivered LAN restores insulin-induced Akt activation in the ARH of DIO mice. **a** Representative photomicrographs (10×) showing pSTAT3 (red) and pAkt (green)-labeled cells 10 min following saline or insulin ip injection (5 U/mouse) in control and DIO mice (scale bar 75 µm, merged image). **b** Graph representing the mean number of ARH neurons displaying pAkt-alone labeling (pAkt-positive/pSTAT3-negative cells) per hemi-section. **c** Representative micrograph (10×) of pSTAT3-labeled (red) and pAkt-labeled (green) neurons after central delivery of LAN followed by insulin ip injection in DIO mice (scale bar 75 µm, merged image). **d** Graph representing the mean number of ARH neurons displaying pAkt/pSTAT3 colabeling per hemi-section. **e** GTT in control and DIO mice following 7 consecutive days of aCSF or LAN (5 mg once daily) icv injections. **f** Area under the curve of the GTT presented in (**e**). All data are represented as mean SEM. ns, $p > 0.05$; * $p < 0.05$; ** $p < 0.01$; *** $p < 0.001$; **** $p < 0.0001$ as one-way ANOVA followed by Tukey's post hoc test (**b**, **c**: $n = 4$–8 mice/group; **e**, **f**: $n = 5/7$ mice/group). See also online supplementary Figure S2. LAN, leptin antagonist; DIO, diet-induced obese; STAT3, signal transducer and activator of transcription; ARH, arcuate nucleus of the hypothalamus.

(Figure continued on next page.)

Fig. 3. Leptin and insulin activate the same pool of ARH neurons. **a** Representative photomicrographs (20×) showing pSTAT3-labeled cells (red) and pAkt-labeled cells (green) following saline, insulin (10 min), leptin (45 min) or leptin + insulin ip injection in lean mice (scale bar 75 µm). **b** Graphs and pie charts representing the mean number of arcuate neurons displaying pSTAT3-alone, pAkt-alone, and colocalized pSTAT3/pAkt labeling per hemi-section after saline, insulin, leptin and leptin + insulin ip injection. **c** Representative photomicrographs (20×) showing pSTAT3 (red) and pAkt (green) labeled cells to illustrate neurons expressing pAkt-alone (green arrows), pSTAT3-alone (red arrows) or colocalized pSTAT3/pAkt (white arrows). **d** Schematic representing the method used for neurons quantification. The top green rectangle illustrates pAkt-labeled neurons quantification on single channel image (green), the top red rectangle illustrates pSTAT3-labeled neurons quantification on single channel image (red), and the green and red rectangles in the bottom illustrate the superposition of both single channel images, with their respective quantification dots pasted in the image, used to quantify pAkt/pSTAT3 colocalizations. Data are represented as mean ± SEM. ** $p < 0.01$; *** $p < 0.001$; **** $p < 0.0001$ as determined by one-way ANOVA followed by Tukey's post hoc test ($n = 4$ mice per group). See also online supplementary Figures S2 and S3.

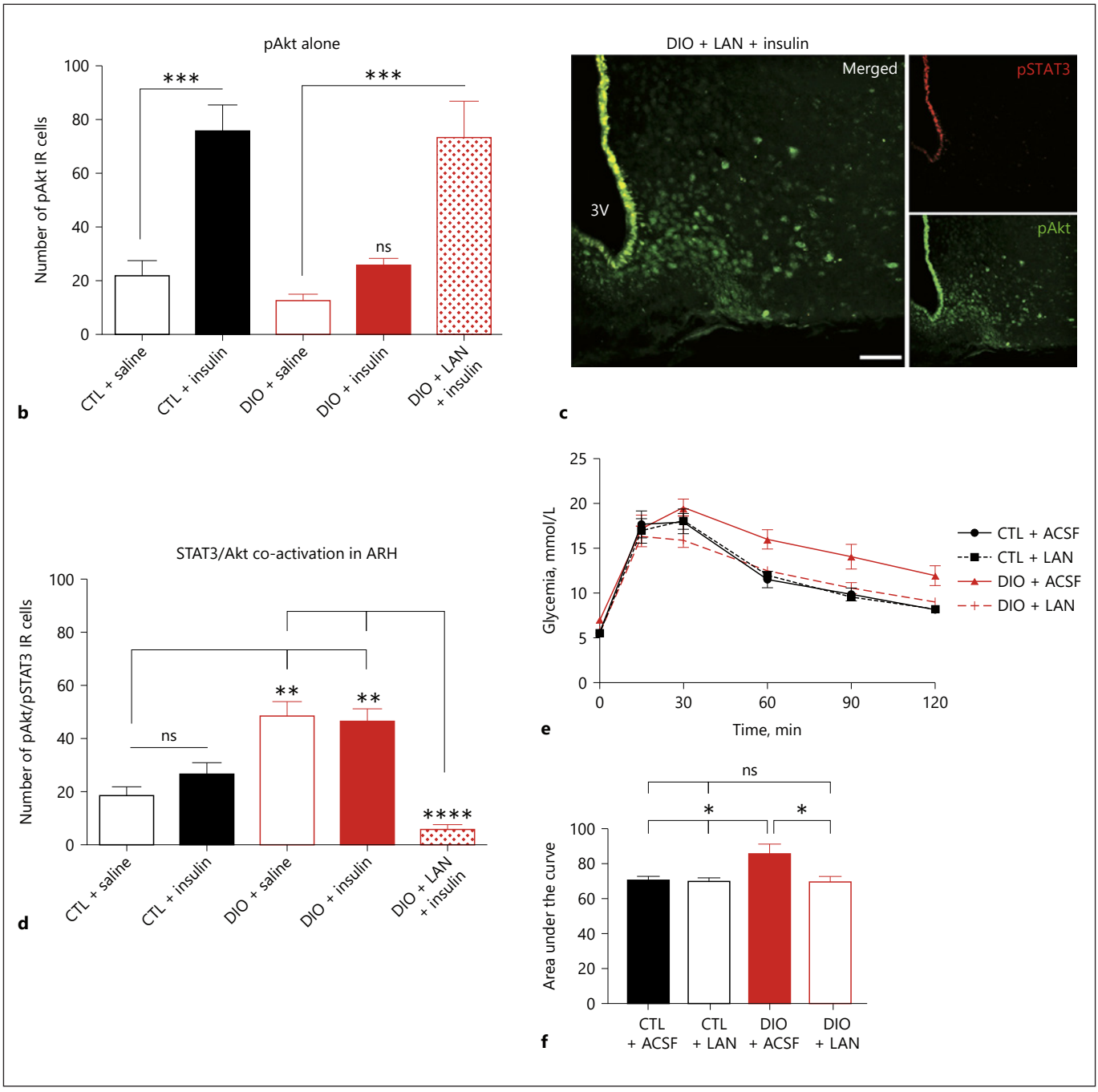

4

rons. Accordingly, we tested if we could improve the neuronal action of insulin by injecting LAN icv before giving insulin peripherally. Strikingly, the level of insulin-induced Akt activation in DIO mice was restored to a similar level observed in control mice (Fig. 4b, c; online suppl. Fig. S2c). This suggests that blocking central leptin signaling improves insulin's capacity to activate Akt in ARH neurons of DIO mice. To investigate whether the rescue of insulin signaling by LAN in DIO mice has a physiological effect on whole-body glucose homeostasis, we performed a GTT following 7 days of icv injections of either ACSF or LAN. In DIO mice, LAN treatment significantly improved glucose tolerance compared to mice given ACSF, proving that central inhibition of leptin signaling was able to normalize the response to glucose challenge in DIO mice (Fig. 4e, f).

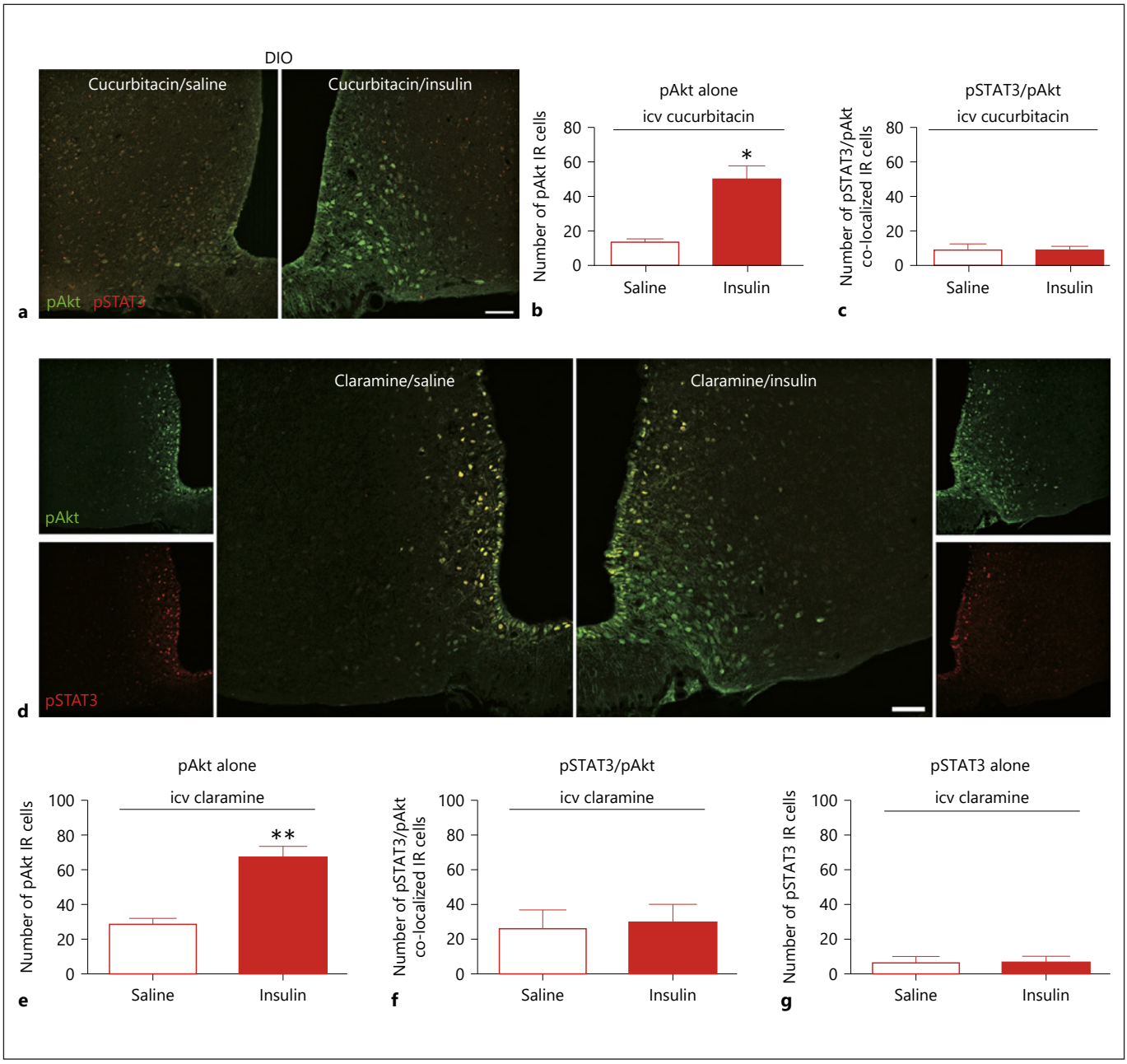

Fig. 5. Central inhibition of JAK/STAT or PTP1B restores insulin-induced Akt activation in the ARH of DIO mice. **a** Representative photomicrographs (20×) showing pSTAT3-labeled cells (red) and pAkt-labeled cells (green) after central delivery of cucurbitacin (5 µg/mouse) followed by saline or insulin ip injection (5 U/mouse) in DIO mice (scale bar 75 µm). **b** Graph representing the mean number of arcuate neurons displaying pAkt-alone labeling (pAkt-labeled/pSTAT3-negative cells) per hemi-section. **c** Graph representing the mean number of arcuate neurons displaying double pAkt/pSTAT3 labeling per hemi-section. **d** Representative photomicrographs (20×) showing pSTAT3-labeled cells (red) and pAkt-labeled cells (green) after central delivery of claramine (5 µg/mouse) followed by saline or insulin ip injection (5 U/mouse) in DIO mice (scale bar 75 µm, merged image). **e** Graph representing the mean number of ARH neurons displaying pAkt-labeling alone (pAkt-positive/pSTAT3-negative cells) per hemi-section. **f** Graph representing the mean number of ARH neurons displaying double-labeling for pAkt and pSTAT3 per hemi-section. **g** Graph representing the mean number of ARH neurons displaying pSTAT3-labeling alone (pSTAT3-positive/pAkt-negative cells) per hemi-section. All data are represented as mean ± SEM. ns, $p > 0.05$; * $p < 0.05$; ** $p < 0.01$ as determined by two-tailed unpaired t test (**b**, **c**: $n = 3$–4 mice/group; **e**–**g**: $n = 3$ mice/group). icv, intracerebro-ventricular; DIO, diet-induced obese.

Next, we used cucurbitacin (5 μg/mouse icv) to inhibit JAK/STAT pathway [25]; it reduced the number of pSTAT3/pAkt colabeled neurons to less than 20 cells per hemi-section in the ARH (Fig. 5a–c). When insulin was administered peripherally following LAN or cucurbitacin icv injection, insulin-induced Akt activation was ~2-fold higher in the ARH of DIO mice and similar to the insulin response observed in control mice (Fig. 4a, b, 5a, b and online suppl. Fig. S2c). These results are consistent with obesity driving increased neuronal LepRb signaling in the ARH to alter neuronal insulin signaling in ARH neurons, resulting in glucose homeostasis alteration.

Pharmacological Inhibition of PTP1B in the CNS Restores Hypothalamic Insulin Signaling Similarly to LepR Antagonism in DIO Mice

PTP1B is part of a feedback loop that negatively regulates leptin and insulin signaling upon receptor activation [21, 26–30]. PTP1B is known to be elevated in the hypothalamus in obesity [28, 31–33]. Since leptin can promote PTP1B expression in response to LepR activation [34], we hypothesized that the persistent activation of Leptin signaling in obesity is associated to a greater PTP1B-mediated inhibition of insulin signaling in the ARH. To test this hypothesis, we investigated in vivo leptin and insulin signaling using immunohistochemistry in conjunction with the icv administration of the PTP1B inhibitor claramine [35]. The number of pAkt-alone labeled neurons in response to insulin (ip) was increased after central PTP1B inhibition (claramine icv) in DIO mice (Fig. 5d–g).

These results suggest that the attenuation of insulin signaling caused by the sustained ARH LepRb signaling is mediated through the induction of PTP1B in DIO mice.

PTP1B Inhibitory Effect on Insulin Signaling is Mediated by AgRP Neurons

AgRP and POMC neurons are 2 major ARH neuronal populations that express high levels of LepRb and InsR. We used triple immunofluorescent labeling to assess leptin and insulin signaling in these neurons. We observed a significant increase in pAkt in AgRP neurons following insulin ip injection (Fig. 6a, c). We found that leptin increased the coactivation of Akt and STAT3 (Fig. 6a, c). Strikingly, the significant increase in Akt-alone activation in response to insulin was lost when leptin was coinjected with insulin while the coactivation of Akt and STAT3 in AgRP neurons remained significantly elevated (Fig. 6a, c). In POMC neurons (marked by γ-MSH labeling), insulin significantly increased Akt-alone activation (Fig. 6b, d). Similarly, leptin increased the coactivation of Akt and STAT3 in POMC neurons (Fig. 6b, d). In contrast to AgRP neurons, both leptin-induced pAkt/pSTAT3 and insulin-induced pAkt-alone remained significantly elevated in POMC neurons when leptin and insulin were coinjected (Fig. 6b, d), highlighting the distinct responses of these types of ARH neurons.

Since leptin seems to influence the insulin response primarily in AgRP neurons, we bred $Ptpn1^{fl/fl}$ (C57Bl/6) mice [21] with Agrp-Ires-Cre mice [22]. The resulting mice failed to express PTP1B specifically in AgRP neurons (AgRP-1B mice). AgRP-1B mice developed diet-in-

Fig. 6. Acute deletion of PTP1B in the AgRP neurons increases insulin sensitivity and ameliorates glucose homeostasis. **a** Representative photomicrographs (10×) showing pAkt-labeled cells (green), pSTAT3-labeled cells (red), and AgRP-labeled cells (magenta) following leptin (45 min) or insulin (10 min) or leptin and insulin ip injection in lean mice (scale bar 75 μm, merged image). **b** Representative photomicrographs (10×) showing pAkt-labeled cells (green), pSTAT3-labeled cells (red), and γ-MSH-labeled cells (magenta) following leptin (45 min) or insulin (10 min) or leptin and insulin ip injection in lean mice (scale bar 75 μm, merged image). **c** Graphs representing the mean number of ARH neurons per hemi-section displaying pSTAT3-labeling in AgRP-labeled neurons, pAkt-labeling in AgRP-labeled neurons, colocalized pSTAT3/pAkt labeling in AgRP-labeled neurons and total number of AgRP-labeled neurons after saline, insulin, leptin and leptin + insulin ip injection. **d** Graphs representing the mean number of ARH neurons per hemi-section displaying pSTAT3-labeling in γ-MSH-labeled neurons, pAkt-labeling in γ-MSH-labeled neurons, colocalized pSTAT3/pAkt labeling in γ-MSH-labeled neurons, and total number of γ-MSH-labeled neurons after saline, insulin, leptin, and leptin + insulin ip injection. **e** Mean body weight of $Ptpn1^{fl/fl}$ and AgRP-1B mice following 16 weeks of high-fat feeding (n = 9–12 mice per group). **f** Mean body fat mass of $Ptpn1^{fl/fl}$ and AgRP-1B mice following 16 weeks of high-fat feeding (n = 9–12 mice per group). **g** Mean body lean mass of $Ptpn1^{fl/fl}$ and AgRP-1B mice following 16 weeks of high-fat feeding (n = 9–12 mice per group). **h** GTT in $Ptpn1^{fl/fl}$ and AgRP-1B mice following 16 weeks of high-fat feeding. **i** Graph showing the mean area under the curve of GTT in $Ptpn1^{fl/fl}$ and AgRP-1B mice following 16 weeks of high-fat feeding. **j** ITT in $Ptpn1^{fl/fl}$ and AgRP-1B mice following 16 weeks of high-fat feeding. **k** Graph showing the mean area under the curve of ITT in $Ptpn1^{fl/fl}$ and AgRP-1B mice following 16 weeks of high-fat feeding. All data are represented as mean ± SEM. ns, $p > 0.05$; * $p < 0.05$; *** $p < 0.001$; **** $p < 0.0001$ as determined by one-way ANOVA followed by Tukey's post hoc test (**c**, **d**: n = 4 mice/group) and two-tailed unpaired t test (**e**–**g**, **i, k**: n = 9–12 mice/group). GTT, glucose tolerance test; ITT, insulin tolerance test.

(For figure see next page.)

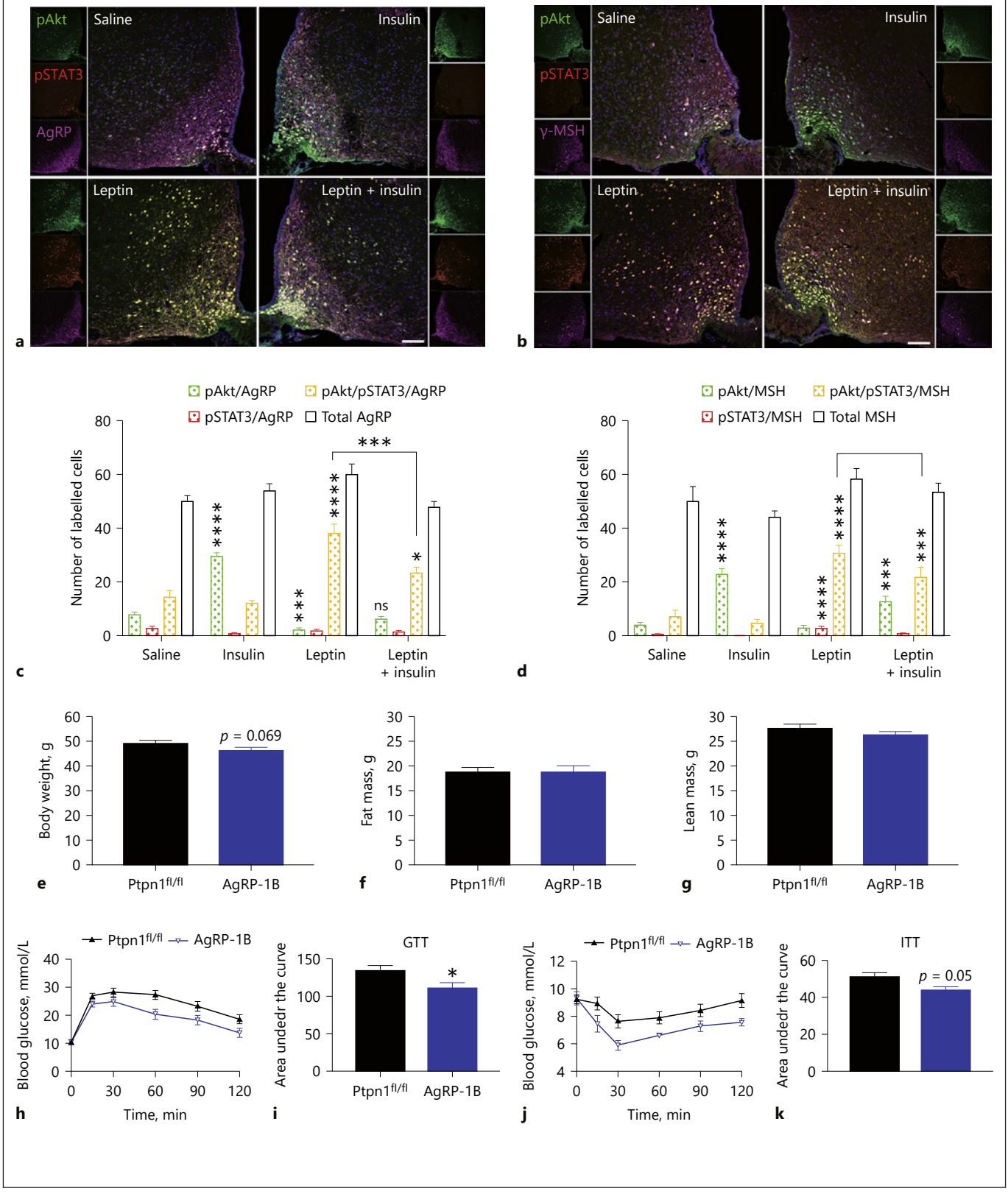

6

duced obesity when fed with HFD during 16 weeks (Fig. 6e). Body weight, fat mass, and lean mass were similar between AgRP-1B mice and $Ptpn1^{fl/fl}$ littermates (Fig. 6e–g). Noteworthy, despite developing diet-induced obesity, AgRP-1B mice displayed a greater tolerance to glucose (Fig. 6h, i) and an improved insulin sensitivity compared to $Ptpn1^{fl/fl}$ mice (Fig. 6j, k). These findings are consistent with leptin signaling inducing PTP1B-mediated repression of insulin signaling in AgRP neurons, resulting in the alteration of glucose homeostasis in obesity.

Discussion

In the current study, we sought to address the hormonal resistance in the hypothalamus associated with obesity. Our results demonstrate an unexplored causal link between leptin and insulin resistance in the hypothalamus of DIO mice. The constant activation of leptin signaling in ARH is responsible, at least in part, for the alteration of hypothalamic insulin signaling and its associated regulation of glucose homeostasis.

In the present study, mice were fed with HFD for a period of 15–20 weeks. We first validated the absence of activation of leptin signaling pathways in response to exogenous leptin administration; a hallmark of cellular leptin resistance, characterized by the absence of leptin-induced increase in pSTAT3-labeled neurons in the ARH. The lack of cellular and physiological response to leptin in DIO mice cannot be explained by an impairment of leptin transport from the blood to the brain. After 8 weeks on HFD, mice do not respond to peripherally injected leptin but the pSTAT3 response to centrally-injected leptin remains intact [36, 37]. Leptin transport can be pharmacologically rescued in 8 weeks DIO mice, allowing the restoration of leptin-induced STAT3 activation in ARH neurons to a level similar to control mice [5]. However, when mice are fed with HFD beyond 12 weeks, there is neither a cellular nor a physiological response to exogenous leptin, even if the hormone is directly injected into the brain.

We observed a high level of STAT3 activation under basal conditions concomitant with resistance to exogenous leptin administration. This event was characterized by an absence of any further increase in the number of pSTAT3-labeled neurons of DIO mice in response to leptin injection compared to basal conditions with no change in body weight, as previously reported [38]. More importantly, our results consistently showed that ARH neurons remained responsive to endogenous leptin. We demonstrated ARH neuronal response to endogenous leptin in DIO by using a competitive LAN in vivo. We also demonstrated an intact cellular response to exogenous leptin treatment in DIO mice using ex vivo hypothalamic slices, a condition that negated the hyperleptinemic environment in DIO mice. Altogether, our results suggest that the response to endogenous leptin remains intact in DIO mice.

Transgenic mice expressing a constitutively active form of STAT3 become obese on HFD [39]. Therefore, constitutive activation of LepRb signaling pathways could be responsible for the lack of physiological effect of exogenous leptin in DIO mice. In this context, understanding the mechanisms of this phenomenon is crucial. The constitutive activation of STAT3 signaling pathway in the ARH neurons of DIO mice has been reported previously [24, 40]. Here we replicated this result but more importantly we demonstrate that DIO mice not only display a constitutive activation of STAT3 signaling but also Akt. Moreover, the activated form of these LepRb-associated signaling molecules colocalized in ARH neurons of DIO mice, and are suppressed by LAN icv injection, suggesting that endogenous leptin itself could be responsible for the high colocalized expression of pSTAT3 and pAkt observed in basal conditions.

Consistent with this notion, Friedman's group elegantly showed that leptin-deficient (*ob/ob*) mice fed a HFD and receiving continuous infusion of leptin to match lean-like leptin levels, remained highly sensitive to leptin [41]. This study suggested that hyperleptinemia, rather than excess adiposity or dietary fats, is necessary to blunt the response to exogenous leptin.

Recently, Ottaway et al. [12] demonstrated that endogenous leptin remains active in DIO mice to regulate food intake and body weight. They show that the administration of a long lasting LAN (PEG-LAN) daily for 7 days induced a similar increase in food intake and body weight in control diet and HFD fed mice. This experiment demonstrates that the effect of endogenous leptin, despite being attenuated (the effect is not as high as the level of endogenous leptin would predict), is still present in DIO animals. However, such effect was absent in leptin deficient (*ob/ob*) and leptin-receptor deficient (*db/db*) mice [12]. In our study, we decided to use a nonpegylated LAN to observe the effect of leptin signaling inhibition on insulin response and glucose homeostasis, in absence of body weight change.

Leptin and insulin are 2 hormones with many common features; both are released into the blood and they

share neuronal targets in the brain [42]. A recent study demonstrated that 50% of arcuate LepR-expressing neurons at least are also responsive to central administration of insulin [43]. Their central actions are deeply involved in the regulation of both energy balance [9, 18, 44, 45] and glucose homeostasis [17, 46–49]. Our data indicate that leptin and insulin can act on the same neuronal population in the ARH and that the sustained activation of lepRb-dependent signaling pathways impairs insulin action on the same neurons in the ARH of DIO mice.

Hypothalamic insulin resistance also occurs in obese humans [50, 51]. The inhibition of central InsR signaling with a competitive insulin-receptor antagonist results in hyperglycemia and glucose intolerance in rats [52], suggesting that the lack of arcuate insulin signaling is involved in the perturbation of systemic glucose homeostasis associated with obesity. We thus build on the premise that the constitutive activation of leptin neuronal targets in DIO mice due to hyperleptinemia prevents further insulin-induced activation of the same ARH neurons involved in glucose homeostasis.

The activation of lepR and insR respectively leads to the activation of a common intracellular signaling cascade, the phospho-inositol-3-kinase/protein kinase B (Akt) pathway, leading to the phosphorylation of Akt on 2 sites: T308 and S473 [53, 54]. Since LepR activation also leads to the phosphorylation of STAT3 [54], we used this dual activation of pSTAT3 and pAkt exerted by LepR to set up a novel immunohistochemistry quantification technique, able to discriminate between leptin-responsive neurons (Akt/STAT3 coactivation) and the insulin-responsive neurons (activation of Akt only).

Using this technique, we show that antagonizing LepRb is capable of rescuing insulin-induced signaling in the ARH of DIO mice. Then, we examined the effect of the rescue of insulin signaling in the ARH on the regulation of glucose homeostasis and observed that DIO mice treated with LAN display a significantly improved tolerance to glucose. These results are consistent with a recent study where we used another paradigm to investigate the effect lepR antagonism on glucose homeostasis. Importantly, we show that the central inhibition of leptin signaling exerted by LAN resulted in the rescue of hepatic glucose production during hyperinsulinemic-euglycemic clamp in DIO mice [63].

Although some studies suggest that insulin transport into the brain is reduced in obese mice [55] and dogs [56], our results suggest that insulin transport persists, at least in part, in DIO mice. In fact, we observe an increase in pAkt levels upon intraperitoneal insulin injection, which demonstrated that exogenous insulin can reach the ARH. However, further investigation is necessary to define the mechanisms of insulin transport.

The constant high level of leptin in the ARH of obese mice is associated with an increased expression of signaling inhibitors such as SOCS3 [57, 58], PTP1B [29, 30, 59], and TCPTP [60]. In standard conditions, these negative regulators are part of a feedback mechanism in response to the activation of the LepRb-dependent signaling cascade. Accordingly, SOCS3 mRNA levels were significantly lower in DIO mice chronically treated with the LAN [12] and PTP1B or TCPTP neuronal deletion enhances leptin sensitivity [21, 60]. However, the persistent activation of LepRb in response to hyperleptinemia makes these feedback mechanisms inefficient in significantly reducing pSTAT3/pAkt levels.

Our data suggest the existence of a cross-talk between leptin and insulin signaling in the ARH. This notion is supported by evidence showing that SOCS3 deletion in LepRb-expressing neurons protects mice from diet-induced insulin resistance independently of body weight [61]. In our study, the persistent activation of lepR in obesity concurrently impairs insulin signaling in neurons that are involved in glucose homeostasis. First, we show that antagonizing LepRb restores insulin-induced signaling in the ARH of DIO mice and is associated with improved glucose tolerance. Then to determine how an increase in LepRb signaling may contribute to hypothalamic insulin resistance in DIO mice, we specifically targeted PTP1B as a potential mediator of this effect. PTP1B expression is induced by leptin signaling [30], and it is a potent negative regulator of insulin signaling, dephosphorylating the InsR and InsR substrate-1 [26–29]. PTP-1B also inhibits leptin signaling [21, 28, 30], the genetic ablation of PTP1B in leptin-responsive neurons results in hypersensitivity to leptin and resistance to diet-induced obesity [62]. Our recent study showed that the elevated level of PTP1B expression in the mediobasal hypothalamus of DIO mice was normalized after 3 days of LAN icv injections [63]. In the present study, central inhibition of PTP1B restores insulin-induced Akt activation in the ARH of DIO mice, similarly to central blockade of leptin signaling. Our observation is supported by the phenotype of the mice lacking PTP1B specifically in neurons. Noteworthy, these animals display increased insulin sensitivity and improved glucose tolerance even on HFD [21].

Since leptin and insulin can act on the same arcuate neuronal populations [43, 45], we hypothesize that persistent leptin signaling in DIO mice could result in enhanced PTP1B activity to blunt insulin signaling in the

ARH neurons involved in glucose homeostasis. We investigated leptin and insulin signaling in the 2 major populations of ARH neurons regulating glucose homeostasis, namely, POMC and AgRP neurons. Our immunohistochemistry studies reveal the convergence of leptin and insulin signaling in AgRP neurons. However, we observe 2 distinctive subpopulations of POMC neurons, which preferentially respond to insulin versus leptin respectively when both hormones are coadministrated. This is consistent with previous findings including the recent single-cell sequencing of POMC neurons, showing the heterogeneity of expression of lepR and InsR in this neuronal population [45, 64, 65]. On the contrary, the heterogeneous response to leptin and insulin did not exist in AgRP neurons. Specifically, the phosphorylation of Akt alone was blunted when leptin and insulin were coinjected while the colocalization of pAkt/pSTAT3 remained elevated. This corresponds to the loss of insulin signaling in AgRP neurons in a context of elevated leptin levels. Furthermore, leptin per se reduces the number of AgRP neurons expressing pAkt-alone, pointing toward a reduced response to endogenous insulin. Overall, these results indicate that prolonged activation of leptin signaling may exert an inhibitory effect via PTP1B on insulin signaling in AgRP neurons, but not in POMC neurons.

Building on this notion, we generated mice deletion of PTP1B specifically in AgRP neurons (AgRP-1B mice). Interestingly, AgRP-1B mice displayed improved glucose tolerance and insulin sensitivity despite their diet-induced obesity, in accordance with our in vivo pharmacological inhibition. This point toward the role of AgRP neurons in the development of hypothalamic insulin resistance associated to obesity and the resulting hyperglycemia.

In conclusion, our findings indicate that the "leptin resistant" state (i.e., no appropriate physiological response) in obese mice is characterized by a persistent response to endogenous leptin at the cellular level. Obesity-induced hyperleptinemia causes the activation of leptin signaling in the ARH neurons, which impairs insulin signaling in AgRP neurons through the induction of PTP1B. Our findings demonstrate that this state of persistent leptin signaling in the ARH underpins the development of hypothalamic insulin resistance, and it accounts, at least in part, for the perturbation of glucose homeostasis in obesity.

Acknowledgments

The authors acknowledge the facilities, scientific, and technical assistance of Monash Micro Imaging, Monash University, Victoria, Australia.

Statement of Ethics

Animal experiments conform to internationally accepted standards and have been approved by the appropriate institutional review body.

Disclosure Statement

The authors have no conflicts of interest to declare.

Funding Sources

This research was supported by a Postdoctoral Fellowship to E.B. from Fondation pour la Recherche Medicale (FRM SPE20140129012), Diabetes Australia Grant to E.B. and M.A.C. (DART Grant 2016). NHMRC Fellowships 1079422 to M.A.C. and 1103037 to T.T., NHMRC Grants 1100240 to M.A.C. and T.T. and Grants 1065641, 1103193 to M.A.C.

Authors Contributions

E.B.: designed and performed the experiments. E.B. and W.C.: wrote the manuscript. M.A.C. and T.T.: supervised the work and edited the manuscript.

References

1 Campfield LA, Smith FJ, Guisez Y, Devos R, Burn P. Recombinant mouse OB protein: evidence for a peripheral signal linking adiposity and central neural networks. Science. 1995 Jul;269(5223):546–9.

2 Zhang Y, Proenca R, Maffei M, Barone M, Leopold L, Friedman JM. Positional cloning of the mouse obese gene and its human homologue. Nature. 1994 Dec;372(6505):425–32.

3 Maffei M, Halaas J, Ravussin E, Pratley RE, Lee GH, Zhang Y, et al. Leptin levels in human and rodent: measurement of plasma leptin and ob RNA in obese and weight-reduced subjects. Nat Med. 1995 Nov;1(11):1155–61.

4 Banks WA, Kastin AJ, Huang W, Jaspan JB, Maness LM. Leptin enters the brain by a saturable system independent of insulin. Peptides. 1996;17(2):305–11.

5 Balland E, Dam J, Langlet F, Caron E, Steculorum S, Messina A, et al. Hypothalamic tanycytes are an ERK-gated conduit for leptin into the brain. Cell Metab. 2014 Feb;19(2):293–301.
6 Tartaglia LA, Dembski M, Weng X, Deng N, Culpepper J, Devos R, et al. Identification and expression cloning of a leptin receptor, OB-R. Cell. 1995 Dec;83(7):1263–71.
7 Scott MM, Lachey JL, Sternson SM, Lee CE, Elias CF, Friedman JM, et al. Leptin targets in the mouse brain. J Comp Neurol. 2009 Jun;514(5):518–32.
8 Robertson SA, Leinninger GM, Myers MG Jr. Molecular and neural mediators of leptin action. Physiol Behav. 2008 Aug;94(5):637–42.
9 Halaas JL, Gajiwala KS, Maffei M, Cohen SL, Chait BT, Rabinowitz D, et al. Weight-reducing effects of the plasma protein encoded by the obese gene. Science. 1995 Jul;269(5223):543–6.
10 Friedman JM, Halaas JL. Leptin and the regulation of body weight in mammals. Nature. 1998 Oct;395(6704):763–70.
11 Frederich RC, Hamann A, Anderson S, Löllmann B, Lowell BB, Flier JS. Leptin levels reflect body lipid content in mice: evidence for diet-induced resistance to leptin action. Nat Med. 1995 Dec;1(12):1311–4.
12 Ottaway N, Mahbod P, Rivero B, Norman LA, Gertler A, D'Alessio DA, et al. Diet-induced obese mice retain endogenous leptin action. Cell Metab. 2015 Jun;21(6):877–82.
13 Simonds SE, Pryor JT, Ravussin E, Greenway FL, Dileone R, Allen AM, et al. Leptin mediates the increase in blood pressure associated with obesity. Cell. 2014 Dec;159(6):1404–16.
14 Elmquist JK, Coppari R, Balthasar N, Ichinose M, Lowell BB. Identifying hypothalamic pathways controlling food intake, body weight, and glucose homeostasis. J Comp Neurol. 2005 Dec;493(1):63–71.
15 Gutiérrez-Juárez R, Obici S, Rossetti L. Melanocortin-independent effects of leptin on hepatic glucose fluxes. J Biol Chem. 2004 Nov;279(48):49704–15.
16 Coppari R, Ichinose M, Lee CE, Pullen AE, Kenny CD, McGovern RA, et al. The hypothalamic arcuate nucleus: a key site for mediating leptin's effects on glucose homeostasis and locomotor activity. Cell Metab. 2005 Jan;1(1):63–72.
17 Berglund ED, Vianna CR, Donato J Jr, Kim MH, Chuang JC, Lee CE, et al. Direct leptin action on POMC neurons regulates glucose homeostasis and hepatic insulin sensitivity in mice. J Clin Invest. 2012 Mar;122(3):1000–9.
18 Brüning JC, Gautam D, Burks DJ, Gillette J, Schubert M, Orban PC, et al. Role of brain insulin receptor in control of body weight and reproduction. Science. 2000 Sep;289(5487):2122–5.
19 Moulton CD, Pickup JC, Ismail K. The link between depression and diabetes: the search for shared mechanisms. Lancet Diabetes Endocrinol. 2015 Jun;3(6):461–71.
20 Spielman LJ, Little JP, Klegeris A. Inflammation and insulin/IGF-1 resistance as the possible link between obesity and neurodegeneration. J Neuroimmunol. 2014 Aug;273(1–2):8–21.
21 Bence KK, Delibegovic M, Xue B, Gorgun CZ, Hotamisligil GS, Neel BG, et al. Neuronal PTP1B regulates body weight, adiposity and leptin action. Nat Med. 2006 Aug;12(8):917–24.
22 Tong Q, Ye CP, Jones JE, Elmquist JK, Lowell BB. Synaptic release of GABA by AgRP neurons is required for normal regulation of energy balance. Nat Neurosci. 2008 Sep;11(9):998–1000.
23 Balland E, Cowley MA. Short-term high-fat diet increases the presence of astrocytes in the hypothalamus of C57BL6 mice without altering leptin sensitivity. J Neuroendocrinol. 2017 Oct;29(10):e12504.
24 Enriori PJ, Sinnayah P, Simonds SE, Garcia Rudaz C, Cowley MA. Leptin action in the dorsomedial hypothalamus increases sympathetic tone to brown adipose tissue in spite of systemic leptin resistance. J Neurosci. 2011 Aug;31(34):12189–97.
25 Boykin C, Zhang G, Chen YH, Zhang RW, Fan XE, Yang WM, et al. Cucurbitacin IIa: a novel class of anti-cancer drug inducing non-reversible actin aggregation and inhibiting survivin independent of JAK2/STAT3 phosphorylation. Br J Cancer. 2011 Mar;104(5):781–9.
26 Galic S, Hauser C, Kahn BB, Haj FG, Neel BG, Tonks NK, et al. Coordinated regulation of insulin signaling by the protein tyrosine phosphatases PTP1B and TCPTP. Mol Cell Biol. 2005 Jan;25(2):819–29.
27 Goldstein BJ, Ahmad F, Ding W, Li PM, Zhang WR. Regulation of the insulin signalling pathway by cellular protein-tyrosine phosphatases. Mol Cell Biochem. 1998 May;182(1-2):91–9.
28 Zhang ZY, Dodd GT, Tiganis T. Protein Tyrosine Phosphatases in Hypothalamic Insulin and Leptin Signaling. Trends Pharmacol Sci. 2015 Oct;36(10):661–74.
29 Elchebly M, Payette P, Michaliszyn E, Cromlish W, Collins S, Loy AL, et al. Increased insulin sensitivity and obesity resistance in mice lacking the protein tyrosine phosphatase-1B gene. Science. 1999 Mar;283(5407):1544–8.
30 Zabolotny JM, Bence-Hanulec KK, Stricker-Krongrad A, Haj F, Wang Y, Minokoshi Y, et al. PTP1B regulates leptin signal transduction in vivo. Dev Cell. 2002 Apr;2(4):489–95.
31 Zabolotny JM, Kim YB, Welsh LA, Kershaw EE, Neel BG, Kahn BB. Protein-tyrosine phosphatase 1B expression is induced by inflammation in vivo. J Biol Chem. 2008 May;283(21):14230–41.
32 Wu Y, Ouyang JP, Wu K, Wang SS, Wen CY, Xia ZY. Rosiglitazone ameliorates abnormal expression and activity of protein tyrosine phosphatase 1B in the skeletal muscle of fat-fed, streptozotocin-treated diabetic rats. Br J Pharmacol. 2005 Sep;146(2):234–43.
33 Dodd GT, Andrews ZB, Simonds SE, Michael NJ, DeVeer M, Brüning JC, et al. A Hypothalamic Phosphatase Switch Coordinates Energy Expenditure with Feeding. Cell Metab. 2017 Aug;26(2):375–393.e7.
34 White CL, Whittington A, Barnes MJ, Wang Z, Bray GA, Morrison CD. HF diets increase hypothalamic PTP1B and induce leptin resistance through both leptin-dependent and -independent mechanisms. Am J Physiol Endocrinol Metab. 2009 Feb;296(2):E291–9.
35 Han Y, Belley M, Bayly CI, Colucci J, Dufresne C, Giroux A, et al. Discovery of [(3-bromo-7-cyano-2-naphthyl)(difluoro)methyl] phosphonic acid, a potent and orally active small molecule PTP1B inhibitor. Bioorg Med Chem Lett. 2008 Jun;18(11):3200–5.
36 Van Heek M, Compton DS, France CF, Tedesco RP, Fawzi AB, Graziano MP, et al. Diet-induced obese mice develop peripheral, but not central, resistance to leptin. J Clin Invest. 1997 Feb;99(3):385–90.
37 El-Haschimi K, Pierroz DD, Hileman SM, Bjørbaek C, Flier JS. Two defects contribute to hypothalamic leptin resistance in mice with diet-induced obesity. J Clin Invest. 2000 Jun;105(12):1827–32.
38 Münzberg H, Myers MG Jr. Molecular and anatomical determinants of central leptin resistance. Nat Neurosci. 2005 May;8(5):566–70.
39 Ernst MB, Wunderlich CM, Hess S, Paehler M, Mesaros A, Koralov SB, et al. Enhanced Stat3 activation in POMC neurons provokes negative feedback inhibition of leptin and insulin signaling in obesity. J Neurosci. 2009 Sep;29(37):11582–93.
40 Martin TL, Alquier T, Asakura K, Furukawa N, Preitner F, Kahn BB. Diet-induced obesity alters AMP kinase activity in hypothalamus and skeletal muscle. J Biol Chem. 2006 Jul;281(28):18933–41.
41 Knight ZA, Hannan KS, Greenberg ML, Friedman JM. Hyperleptinemia is required for the development of leptin resistance. PLoS One. 2010 Jun;5(6):e11376.
42 Belgardt BF, Brüning JC. CNS leptin and insulin action in the control of energy homeostasis. Ann N Y Acad Sci. 2010 Nov;1212(1):97–113.
43 Garcia-Galiano D, Borges BC, Donato J Jr, Allen SJ, Bellefontaine N, Wang M, et al. PI3Kα inactivation in leptin receptor cells increases leptin sensitivity but disrupts growth and reproduction. JCI Insight. 2017 Dec;2(23):96728.
44 Woods SC, Lotter EC, McKay LD, Porte D Jr. Chronic intracerebroventricular infusion of insulin reduces food intake and body weight of baboons. Nature. 1979 Nov;282(5738):503–5.
45 Dodd GT, Decherf S, Loh K, Simonds SE, Wiede F, Balland E, et al. Leptin and insulin act on POMC neurons to promote the browning of white fat. Cell. 2015 Jan;160(1–2):88–104.

46 Obici S, Zhang BB, Karkanias G, Rossetti L. Hypothalamic insulin signaling is required for inhibition of glucose production. Nat Med. 2002 Dec;8(12):1376–82.
47 Pocai A, Morgan K, Buettner C, Gutierrez-Juarez R, Obici S, Rossetti L. Central leptin acutely reverses diet-induced hepatic insulin resistance. Diabetes. 2005 Nov;54(11):3182–9.
48 Hill JW, Elias CF, Fukuda M, Williams KW, Berglund ED, Holland WL, et al. Direct insulin and leptin action on pro-opiomelanocortin neurons is required for normal glucose homeostasis and fertility. Cell Metab. 2010 Apr;11(4):286–97.
49 Fujikawa T, Berglund ED, Patel VR, Ramadori G, Vianna CR, Vong L, et al. Leptin engages a hypothalamic neurocircuitry to permit survival in the absence of insulin. Cell Metab. 2013 Sep;18(3):431–44.
50 Heni M, Kullmann S, Preissl H, Fritsche A, Häring HU. Impaired insulin action in the human brain: causes and metabolic consequences. Nat Rev Endocrinol. 2015 Dec;11(12):701–11.
51 Heni M, Wagner R, Kullmann S, Veit R, Mat Husin H, Linder K, et al. Central insulin administration improves whole-body insulin sensitivity via hypothalamus and parasympathetic outputs in men. Diabetes. 2014 Dec;63(12):4083–8.
52 Vikram A, Jena G. S961, an insulin receptor antagonist causes hyperinsulinemia, insulin-resistance and depletion of energy stores in rats. Biochem Biophys Res Commun. 2010 Jul;398(2):260–5.
53 Plum L, Schubert M, Brüning JC. The role of insulin receptor signaling in the brain. Trends Endocrinol Metab. 2005 Mar;16(2):59–65.
54 Niswender KD, Schwartz MW. Insulin and leptin revisited: adiposity signals with overlapping physiological and intracellular signaling capabilities. Front Neuroendocrinol. 2003 Jan;24(1):1–10.
55 Urayama A, Banks WA. Starvation and triglycerides reverse the obesity-induced impairment of insulin transport at the blood-brain barrier. Endocrinology. 2008 Jul;149(7):3592–7.
56 Kaiyala KJ, Prigeon RL, Kahn SE, Woods SC, Schwartz MW. Obesity induced by a high-fat diet is associated with reduced brain insulin transport in dogs. Diabetes. 2000 Sep;49(9):1525–33.
57 Bjørbaek C, Elmquist JK, Frantz JD, Shoelson SE, Flier JS. Identification of SOCS-3 as a potential mediator of central leptin resistance. Mol Cell. 1998 Mar;1(4):619–25.
58 Münzberg H, Flier JS, Bjørbaek C. Region-specific leptin resistance within the hypothalamus of diet-induced obese mice. Endocrinology. 2004 Nov;145(11):4880–9.
59 Klaman LD, Boss O, Peroni OD, Kim JK, Martino JL, Zabolotny JM, et al. Increased energy expenditure, decreased adiposity, and tissue-specific insulin sensitivity in protein-tyrosine phosphatase 1B-deficient mice. Mol Cell Biol. 2000 Aug;20(15):5479–89.
60 Loh K, Fukushima A, Zhang X, Galic S, Briggs D, Enriori PJ, et al. Elevated hypothalamic TCPTP in obesity contributes to cellular leptin resistance. Cell Metab. 2011 Nov;14(5):684–99.
61 Pedroso JA, Buonfiglio DC, Cardinali LI, Furigo IC, Ramos-Lobo AM, Tirapegui J, et al. Inactivation of SOCS3 in leptin receptor-expressing cells protects mice from diet-induced insulin resistance but does not prevent obesity. Mol Metab. 2014 Jun;3(6):608–18.
62 Tsou RC, Zimmer DJ, De Jonghe BC, Bence KK. Deficiency of PTP1B in leptin receptor-expressing neurons leads to decreased body weight and adiposity in mice. Endocrinology. 2012 Sep;153(9):4227–37.
63 Balland E, Chen W, Dodd GT, Conductier G, Coppari R, Tiganis T, et al. Leptin Signaling in the Arcuate Nucleus Reduces Insulin's Capacity to Suppress Hepatic Glucose Production in Obese Mice. Cell Rep. 2019 Jan 8;26(2):346–355.e3.
64 Lam BY, Cimino I, Polex-Wolf J, Nicole Kohnke S, Rimmington D, Iyemere V, et al. Heterogeneity of hypothalamic pro-opiomelanocortin-expressing neurons revealed by single-cell RNA sequencing. Mol Metab. 2017 Mar;6(5):383–92.
65 Williams KW, Margatho LO, Lee CE, Choi M, Lee S, Scott MM, et al. Segregation of acute leptin and insulin effects in distinct populations of arcuate proopiomelanocortin neurons. J Neurosci. 2010 Feb;30(7):2472–9.